https://doi.org/10.5194/gmd-2020-12
Preprint. Discussion started: 3 March 2020

Geoscientific Model Development Discussions

Effects of spatial resolution on WRF v3.8.1 simulated meteorology over the central Himalaya

Jaydeep Singh[1], Narendra Singh[1*], Narendra Ojha[2], Amit Sharma[3, a], Andrea Pozzer[4, 5*], Nadimpally Kiran Kumar[6], Kunjukrishnapillai Rajeev[6], Sachin S. Gunthe[3], V. Rao Kotamarthi[7]

[1]Aryabhatta Research Institute of Observational Sciences, Nainital, India

[2]Physical Research Laboratory, Ahmedabad, India

[3]EWRE Division, Department of Civil Engineering, Indian Institute of Technology Madras, Chennai, India

[4]Department of Atmospheric Chemistry, Max Planck Institute for Chemistry, Mainz, Germany

[5]Earth System Physics Section, International Centre for Theoretical Physics, Trieste, Italy

[6]Space Physics Laboratory, Vikram Sarabhai Space Centre, Thiruvananthapuram, India

[7]Environmental Science Division, Argonne National Laboratory, Argonne, Illinois, USA

[a]Now at Laboratory for Atmospheric Research, Washington State University, Pullman, WA, USA

Correspondence: Narendra Singh (narendra@aries.res.in) and Andrea Pozzer (andrea.pozzer@mpic.de)

Abstract

The sensitive and fragile ecosystem of the central Himalayan (CH) region, experiencing enhanced anthropogenic pressure, requires adequate atmospheric observations and an improved representation of Himalaya in the models. However, the accuracies of atmospheric models remain limited here due to highly complex mountainous topography. This article delineates the effects of spatial resolution on the modeled meteorology and dynamics over the CH by combining the WRF (Weather Research and Forecasting) model with the GVAX (Ganges Valley Aerosol Experiment) observations during the summer monsoon. WRF simulation is performed over a domain (d01) encompassing northern India at 15 km x 15 km resolution, and two nests: d02 (5 km x 5 km) and d03 (1 km x 1 km) centered over CH with boundary

https://doi.org/10.5194/gmd-2020-12
Preprint. Discussion started: 3 March 2020

conditions from respective parent domains. WRF simulations reveal higher variability in meteorology e.g. Relative Humidity (RH=71.4–93.3%), Wind speed (WS=1.6–3.1 ms^{-1}), as compared to the ERA Interim reanalysis (RH=79.4–85.0, and WS=1.3–2.3ms^{-1}) over the northern India owing to higher resolution. WRF simulated temporal evolution of meteorological profiles is seen to be in agreement with the balloon-borne measurements with stronger correlations aloft (r = 0.44–0.92), than those in the lower troposphere (r = 0.27–0.48). However, the model overestimates temperature (warm bias by 2.8°C) and underestimates RH (dry bias by 7.6%) at surface in the d01. Model results show a significant improvement in d03 (P=827.6 hPa, T=19.8°C, RH=90.2%) and are closer to the GVAX observations (P=801.3, T=19.5, RH=94.5%). Temporal variations in near surface P, T and RH are also reproduced by WRF d03 to an extent (r > 0.5). A sensitivity simulation incorporating the feedback from nested domain demonstrated improvements in simulated P, T and RH over CH. Our study shows the WRF model set up at finer spatial resolution can significantly reduce the biases in simulated meteorology and such an improved representation of CH can be adopted through domain feedback into regional-scale simulations. Interestingly, WRF simulates a dominant easterly wind component at 1 km x 1 km resolution (d03), which was missing in the coarse simulations; however, a frequent southeastward wind component remained underestimated. Model simulation implementing a high resolution (3 s) topography input (SRTM) improved the prediction of wind directions, nevertheless, further improvements are required to better reproduce the observed local-scale dynamics over the CH.

1. Introduction

Himalayan region is one of the most complex and fragile geographical systems in the world, and has paramount importance for the climatic implications and air composition at regional to global scales (e.g. Lawrence et al., 2010, Pant et al., 2018; Lelieveld et al., 2018). The ground-based observations of meteorology and fine-scale dynamics are highly sparse. In this direction, an intensive field campaign called as the GVAX (Kotamarthi, 2013) was carried out over a mountainous site in the Central Himalaya which provided valuable meteorological observations for atmospheric research, model evaluation and improvements. Accurate simulations of meteorology are needed for numerous investigations, such as to study the regional and global climate change, snow-cover change, trapping and transport of regional pollution, and the hydrological cycle especially monsoon system (e. g. Sharma and Ganju, 2000; Bhutiyani et al., 2007; Pant et al., 2018). Studies focussing over this region have become more important due to the increasing anthropogenic influences resulting in enhanced levels of Short-Lived Climate forcing Pollutants (SLCPs) along the Himalayan foothills (e. g. Ojha et al., 2012; Sarangi et al., 2014; Rupakheti et al., 2017; Deep et al., 2019; Ojha et al., 2019). Although Global Climate Models (GCMs) simulate the climate variabilities over global scale, their application for reproducing observations in the regions of complex landscapes is limited, due to coarse horizontal resolution (e. g. Wilby et al., 1999; Boyle et al. 2010; Tselioudis et al., 2012; Pervez and Henebry, 2014; Meher et al., 2017). Mountain ridges, rapidly changing land-cover, and the low altitude valleys often lie within a grid box of typical global climate models resulting in significant biases in model results when compared with observations (e. g. Ojha et al., 2012; Tiwari et al., 2017, Pant et al., 2018). On the other hand, Regional Climate Models (RCMs) at finer resolutions allow better representation of the topographical features thus providing improved simulations of the atmospheric variability over regions of complex terrains. Several mesoscale models (e. g. Christensen et al., 1996; Caya and Laprise 1999; Skamarock et al., 2008; Zadra et al., 2008) have been developed and applied successfully over different parts of the world. These studies have revealed that the RCMs provide significant new insights by parameterizing or explicitly simulating atmospheric processes over finer spatial scales. Nevertheless, large uncertainties are still seen over highly complex areas indicating the effects of further unresolved terrain features (e. g. Wang et al., 2004; Laprise, 2008; Foley, 2010) and need to improve the simulations.

Of late, anthropogenic influences and climate forcing have been increasing over the Himalaya and its foothill regions since pre-industrial times (Pant et al., 2006; Bonasoni et al., 2012; Srivastava et al., 2015). Further, an increase in the intensity and frequency of extreme weather events have been observed over the

https://doi.org/10.5194/gmd-2020-12
Preprint. Discussion started: 3 March 2020

Himalayan region (e. g. Nandargi and Dhar, 2012; Sun et al., 2017; Dimri et al., 2017) in past few decades. These events include extreme rainfall and resulting flash floods, cloudbursts, landslides etc., and their causes range from mesoscale processes to larger synoptic scale events. Unfortunately, the lack of observational network covering the Himalaya and foothills with sufficient spatio-temporal density inhibits the detailed understanding of the aforementioned processes, and meteorological and dynamical conditions in the region. Therefore, usage of regional models, evaluated against available in-situ measurements would fill the gap of investigating atmospheric variability in the observationally sparse and geographically complex terrain of Himalaya.

In this regard, a few studies have applied the regional model WRF to simulate the variations in the meteorology, winds, and boundary layer dynamics over the Himalaya and foothills (Kumar et al., 2012; Sarangi et al., 2014; Singh et al., 2016; Mues et al., 2018). WRF model with suitably chosen schemes is generally able to reproduce the spatio-temporal variations in the regional-scale meteorology and wind patterns (Kumar et al., 2012) and to an extent also captured the mountain-valley wind systems (Sarangi et al., 2014) and boundary layer dynamics (Singh et al., 2016; Mues et al., 2018). However, most of these studies utilized model at horizontal resolutions of 45 to 30 km, except study by Singh et al. (2016) used relatively higher spatial resolution (5 km x 5 km). Nevertheless, it remains unclear how the finer resolution could better resolve the complex terrain of the central Himalaya and improve the meteorological simulations, especially at 5 km to 1 km resolution.

With this opportunity of model evaluation and improvements in simulating meteorological and dynamical variability over the CH, here, we have used a nested WRF set up with a coarse 15 km x 15 km domain (d01) with nests of 5 km x 5 km (d02) and 1 km x 1 km (d03) centred over the CH. The main objectives of the study are as follows:

1. To examine the model performance over the CH at 15 km x 15 km resolution

https://doi.org/10.5194/gmd-2020-12
Preprint. Discussion started: 3 March 2020

2. To examine the effects or improvements that can be achieved at higher spatial resolutions: 5 km x 5 km, and 1 km x 1 km.
3. To investigate the effect of feedback from nest that could be adopted into parent domain, as this would allow configuring a setup covering larger Indian region with more accurate results over Himalaya
4. To implement a very high resolution (3 s) topographical input into the model to examine the potential of simulations finer than 1 km in reproducing local-scale dynamics

Subsequent section 2 describes the model set up, followed by experimental design, and a discussion of datasets used for model evaluation. Section 3 provides comparison of model results with the ERA Interim reanalysis (section 3.1), radiosonde observations (section 3.2), and ground-based measurements (section 3.3). Analysis of domain feedback is presented in section 3.4, and the effect of implementing high resolution topography is investigated in section 3.5, followed by the summary and conclusions in the section 4.

2. Methodology

2.1 Model set up and Experimental Design

Weather Research and Forecasting (WRF) model–version 3.8.1 has been used in the present study. WRF is a mesoscale non-hydrostatic, Numerical Weather prediction (NWP) model with advance physics and numerical schemes for simulating meteorology and dynamics. WRF-ARW uses Eulerian mass based dynamical core with terrain-following vertical coordinates (Skamarock et al., 2008). ERA Interim reanalysis from the European Center for Medium Range Weather Forecasts (ECMWF) available at a horizontal resolution of 0.7^0 x 0.7^0 at 6 h interval has been used to provide the initial and lateral boundary conditions to the WRF model. Static geographical data, which includes the information of terrain height, land use, and land cover etc., is based on the Moderate Resolution Imaging Spectroradiometer (MODIS) data available at 30s horizontal resolution.

https://doi.org/10.5194/gmd-2020-12
Preprint. Discussion started: 3 March 2020

Geoscientific Model Development Discussions
Open Access
EGU

The shortwave radiation scheme used is the Goddard scheme (Chou and Suarez, 1994) while the long wave radiation is simulated by the Rapid Radiative Transfer Model (Mlawer et al., 1997) scheme. For resolving the boundary layer processes the first order nonlocal closure based Yonsei University (YSU) scheme (Hong et al., 2006) is used including an explicit entrainment layer with the K-profile in an unstable mixed layer. PBL height is determined from the Richardson number (Ri_b) method in this PBL scheme. Convection is parameterized by the Kain-Fritsch (KF) cumulus parameterization (CP) scheme, accounting for sub-grid level processes in the model such as precipitation, latent heat release and vertical redistribution of heat and moisture as a result of convection (Kain, 1990). With increase in model grid resolution to less than 10 km (known as "grey area"), the CP scheme is usually turned off and an explicit microphysics (MP) scheme is needed to resolve cloud and precipitation processes (Weisman et al., 1997). In the present study, the CP scheme is used for d01 while it is turned off for d02 and d03. The Thomson microphysics containing prognostic equations for cloud water, rain water, ice, snow, and graupel mixing ratios, is used (Thompson et al., 2004). Parameterization of surface processes is done with MM5 Monin-Obukhov scheme and Unified Noah land surface model (LSM) (Chen and Dudhia, 2001; Ek et al., 2003; Tewari et al., 2004). The Noah LSM includes a single canopy layer and four soil layers at 0.1, 0.2, 0.6 and 1m within 2m of depth (Ek et al., 2003).

The model is configured with three domains of 15 km (d01), 5 km (d02) and 1 km (d03) horizontal grid spacing using Mercator projection centering at Manora Peak (79.46^{o}N, 29.36^{o}E, amsl ~ 1958m) in central Himalaya. Topography within the model domains is highly complex as evident form the ridges (Figure 1). Outer domain d01 includes north part of Thar Desert, part of IGP (Indo-Gangetic-Plain), Himalayan mountains with vegetation and snow cover, while the innermost domain d03 consists of mostly mountainous terrain. Model atmosphere has 51 vertical levels with top at 10 hPa. For d01, 100 east-west and 86 north south grid points are used to account for the effect of synoptic scale meteorology e.g. Indian summer monsoon. The d02 has 88 east-west and 76 north-south grid points covering sufficient spatial region around the observational site to consider the effects of mesoscale dynamics, e.g. change of wind

https://doi.org/10.5194/gmd-2020-12
Preprint. Discussion started: 3 March 2020

pattern due to orography. The innermost domain 03 has 126 east-west and 106 north-south grid points mainly to reveal local effects e.g. convection, advection, turbulence, orthographic lifting etc.

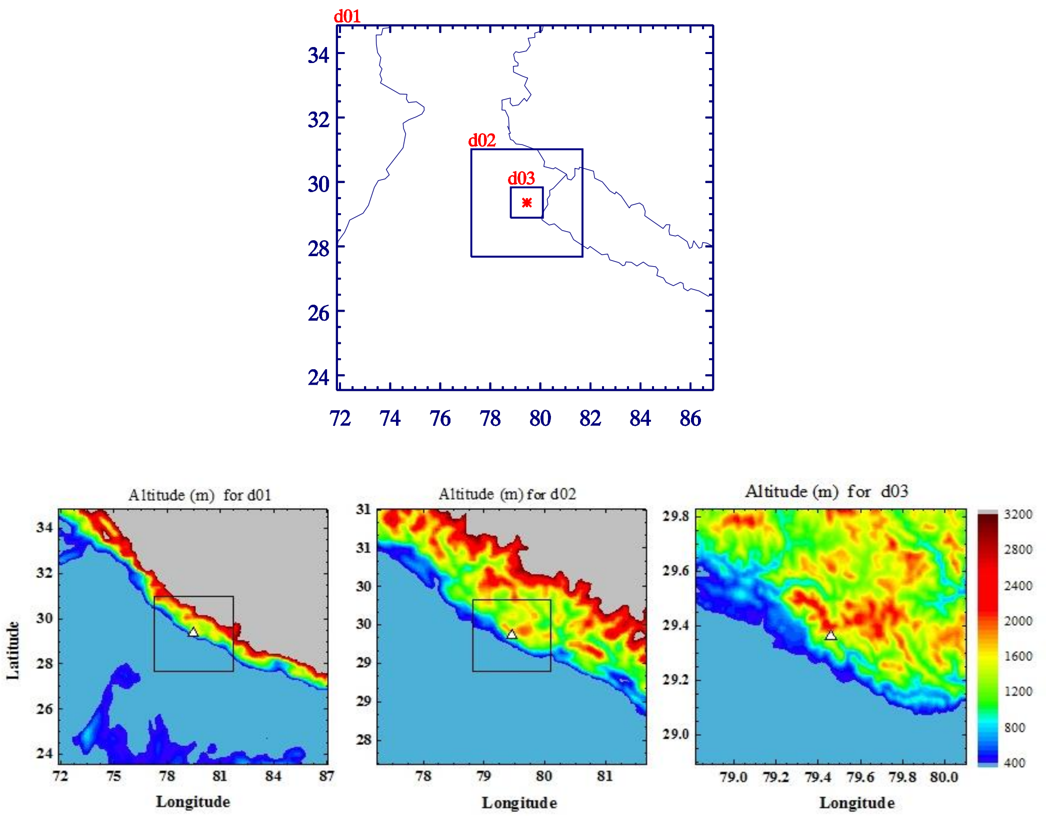

Figure 1: Topography in WRF model domains at three horizontal resolutions: domain d01 (15 x 15km), domain d02 (5 x 5km) and domain d03 (1 x 1 km). Triangle sign indicates the location of the GVAX campaign over Manora Peak, Nainital. Box inside the figure represents the nested domain.

The d01 simulation provides the boundary conditions to domain d02, and domain d02 to innermost domain d03. For d01, boundary conditions are provided from ERA Interim reanalysis, as explained earlier. Model simulation has been performed for four months of the summer monsoon season: 01 June 2011 to 30 September 2011 (JJAS). First 10 days of the simulation is considered as the spin-up and removed from the analysis. Only the outer domain d01 is nudged with the global reanalysis for temperature, water vapor,

https://doi.org/10.5194/gmd-2020-12
Preprint. Discussion started: 3 March 2020

Geoscientific Model Development Discussions
Open Access

zonal and meridional (u and v) components of wind with nudging coefficient of 0.0006 (6 x 10^{-4}) at all vertical levels (e.g. Kumar et al., 2012). Several of the configuration options e. g. physics, meteorological nudging, etc. are selected following earlier applications of this model over this region (e. g. Kumar et al., 2012; Ojha et al., 2016; Singh et al., 2016; Sharma et al., 2017).

2.2. Observational data

We utilize the observations conducted as a part of an intensive field campaign- the Ganges Valleys Aerosol Experiment (GVAX) for the evaluation of model simulations. The GVAX campaign was conducted using Atmospheric Radiation Measurement (ARM) Climate Research Facility of the U.S. Department of Energy (DOE) from June, 10 2011 to March 31, 2012 at ARIES, Manora Peak in Nainital (e.g. Kotamarthi, 2013; Singh et al., 2016; Naja et al., 2016). The surface-based meteorological measurements of ambient air temperature, pressure, relative humidity, precipitation, wind (speed and direction) were carried out using an automatic weather station at 1-minute temporal resolution.

The vertical profiles of temperature, pressure, relative humidity and horizontal wind (speed and direction) were measured by four launches (00:00, 06:00, 12:00 and 18:00 UTC) of the radiosonde each day during the campaign (Naja et al., 2016). The continuous vertical profiles of the meteorological parameters except wind speed and direction were available from end of June 2011 to the entire period of study, whereas valid wind data were available only for September 2011. Hence, in this study, radiosonde measurements from July 1, 2011 onwards are used for model evaluation of meteorological parameters, except wind speed and direction, which are evaluated for the month of September.

3. Results and Discussions

3.1. Comparison with ERA Interim reanalysis

ERA Interim reanalysis data set is available globally at resolution of 0.75^0 x 0.75^0 with 60 vertical levels from surface to the top at 0.1 hPa with covering time period from 1979 to present at 6-hourly time step

https://doi.org/10.5194/gmd-2020-12
Preprint. Discussion started: 3 March 2020

(Dee et. al., 2001). Re-gridded ERA-Interim data are also available at various resolutions such as 0.125, 0.25, 0.50, 0.75, 1.0 etc. Here, we have used the highest resolution data available at 0.125° x 0.125° for comparison with WRF results. We first compare the WRF simulated spatial distribution of meteorological parameters (surface pressure, 2m air Temperature, 2m RH and 10m WS) with ERA Interim reanalysis over common area of all the domains and averaged for the complete simulation period (Figure 2). The common area in all domains includes low-altitude Indo-Gangetic Plain (IGP) region in south (with elevation of less than 400m, Figure 1) and elevated mountains of the central Himalaya in north. Also, for a consistent comparison, model simulated values are taken at the same time intervals as that in ERA Interim data (i.e. every 6h). From the comparison (Figure 2), it is evident that the meteorological parameters simulated by the model are dependent on the model grid resolution. The existence of the sharp gradient topographic height (SGTH) of about 1600 m from the foothill of the Himalaya to the observational site modifies the wind pattern as well as moisture content differently at different grid resolutions, indicating the critical role of mountain orography. The surface pressure explicitly depends upon the elevation of a location from mean sea level. The contour plot of the pressure from ERA Interim shows surface pressure of about 883.9 hPa for observational site Manora Peak, while WRF simulated pressure is 839 hPa, 821hPa and 840 hPa for d03, d02 and d01, respectively. WRF simulated surface pressure ranges from 829.0 hPa over high altitude CH region to 979.5 hPa in IGP region within d01. At the same time, the variation range of surface pressure is 817.0–978.8 and 795–977.6 hPa within d02 and d03 respectively, and this is attributed to the improvement in resolved topography on increasing model grid resolution. The effects of the SGTH are not clearly observed for temperature, wind and RH in ERA-Interim contours, and it could be due to the unresolved topographic features. Simulated spatial profiles show significantly distinct meteorology in Indo-Gangetic Plain (IGP), which lies just in the foothills of Himalaya, and elevated central Himalayan region.

https://doi.org/10.5194/gmd-2020-12
Preprint. Discussion started: 3 March 2020

Geoscientific Model Development Discussions
Open Access
EGU

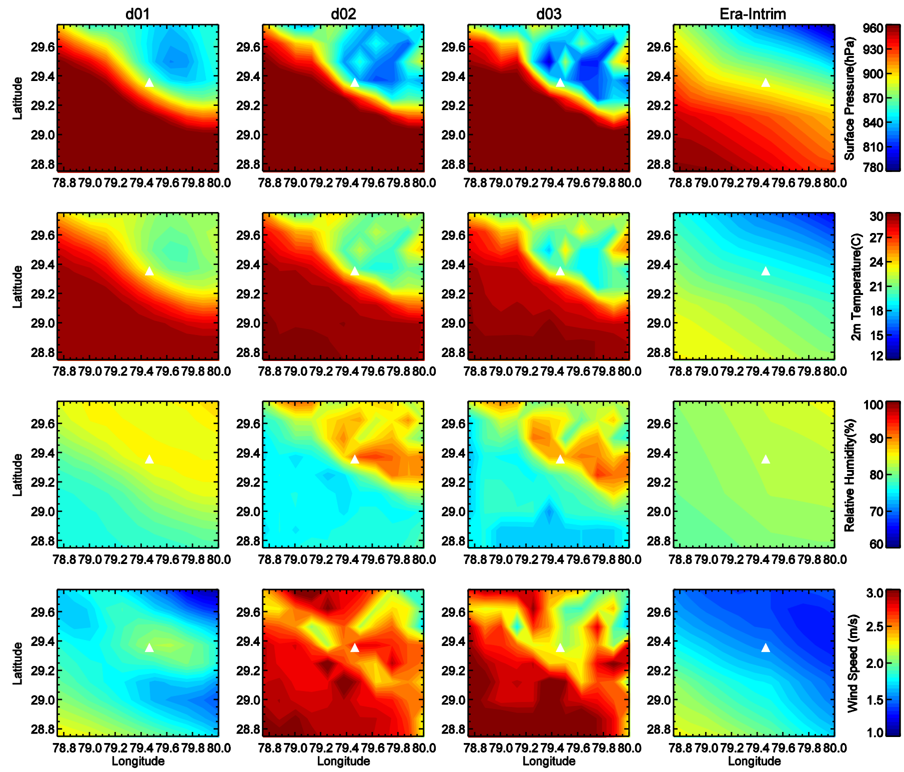

Figure 2:. Contours in the first three columns show WRF results and the fourth column shows corresponding parameters from the ERA Interim reanalysis. First row shows mean surface pressure during the monsoon (JJAS), second row shows 2m temperature, 3rd row shows 2m relative humidity (RH) and bottom row shows 10 m wind speed.

The effect of spatial resolution is clearly observed over the mountainous region of Himalaya, where size of the mountains changes abruptly, with the modelled output showing distinct features with increasing grid resolution. On the other hand, there are minimal differences in the topography of the IGP, and hence features are well captured in the model even at coarser resolution of 15 Km.

Model simulations show topography dependent spatial variation in the 2m temperature in the ranges of 20.2–29.6^{0}C in d01,19.2–29.8^{0}C in d02, and 18.0–29.8^{0}C in d03 with lowest values simulated over the

https://doi.org/10.5194/gmd-2020-12
Preprint. Discussion started: 3 March 2020

Geoscientific Model Development Discussions
Open Access EGU

elevated mountain peaks and higher values over the temperate IGP region. The contours in three model domains show explicit dependency of 2m temperature on the grid resolution over the mountainous region. With increasing model resolution, the topography is resolved to a greater extent and the lower temperature is simulated at higher surface elevations, as expected. Estimation of water vapour is very important for both climate and numerical weather prediction (NWP) applications. The relative humidity is above 70% in all three domains as the study period is monsoon season. The variations (minimum-maximum) in the humidity in ERA-Interim (80% to 85%) data sets, domains d01 (76-87%), d02 (73 – 93%), and d03 (71-93%) are generally comparable. The mountain slopes provide the uplift to the monsoonal moist air that subsequently saturates on ascent and increases the relative humidity to about 90% as observed over the grid encompassing the site.

The wind speed is highly dependent upon the model grid resolution as well as orography-induced circulations during different seasons (Solanki et al., 2016; Solanki et al 2019) as shown in Fig. 2. As mentioned earlier, although the topography of the IGP region does not vary abruptly, the magnitude of the wind speed over this region as well as over the complex Himalayan region are found to change significantly at different model resolutions, thereby indicating that the wind speed is very sensitive to both model resolution and topography. The wind speed in d01 varies from minimum value of 1.1 ms^{-1} to maximum value of 2.3 ms^{-1} and agrees better with the ERA-Interim dataset (1.3 ms^{-1} to 2.3 ms^{-1}), while the wind variations in domains d02 and d03 (1.6 to 3.1 ms^{-1}) are similar but are overestimated as compared to the ERA-interim.

3.2. Comparison with Radiosonde observations

The vertical profiles of the meteorological parameters: temperature, relative humidity and wind speed are from surface to 50 hPa are shown in the Figure 3 for WRF-d01 simulation and the radiosonde observations. As mentioned earlier, the snapshots of atmospheric profiles are obtained using radiosondes launched four

https://doi.org/10.5194/gmd-2020-12
Preprint. Discussion started: 3 March 2020

Geoscientific Model Development
Discussions

times a day during the GVAX campaign. Various features of the temperature profiles are seen to be well simulated by the WRF model (Figure 3).

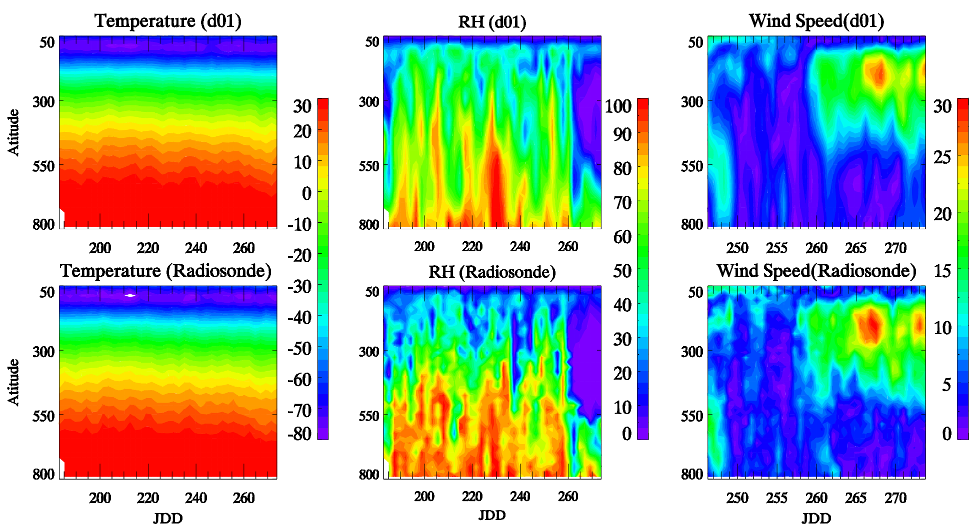

Figure 3: The comparison of WRF simulated temperature, relative humidity and wind speed vertical profiles with the radiosonde observations for the pressure-levels from 800 hPa to 50 hPa. Horizontal axis shows the day number of the year 2011 (JDD) starting from 1 July (182th day) to 30 September (273th day). Wind speed profiles are plotted only for month September, 2011.

The inversion of the temperature at the top of the troposphere occurred at ~100hPa (~16km) in observations, while it occurred at slightly higher altitude (~80hPa) in the model for domain d01. Further WRF model simulates wetter (or more humid) atmosphere at higher altitudes while showing a good agreement with the observations of water content in lower altitudes. The observations of wind speed were available only from 01 September 2011 onwards therefore wind comparison is made only for the September month. The simulated profiles of the wind agree generally well with the observations. For the statistical comparison of the simulated meteorology with the observations, the Taylor diagram (Taylor, 2001) is used and shown in Figure 6. In the diagram the comparison is summarized with correlation

https://doi.org/10.5194/gmd-2020-12
Preprint. Discussion started: 3 March 2020

coefficient (r), normalized root mean squared difference (RMSD) and normalized standard deviation (SD), normalized to the standard deviation of observation. In most of the cases (shown in Figure 6a) model simulates less variability in meteorological parameters as shown by the normalized standard deviation which turns out to be less than 1. For temperature and wind speed, model shows good agreement at 250hPa ($r > 0.90$) than that in lower altitudes i.e. 750hPa ($r < 0.42$). On the other hand, model captures variability in humidity relatively well at 500 hPa ($r = 0.71$) but shows poor correlation at 50 hPa ($r = 0.17$) near the model top. Lower correlations for temperature and wind speed at 750 hPa pressure near the surface could be due to the terrain induced effects most significant in the local boundary layer. The, surface level winds, and turbulence etc. are some of the features of the boundary layer that are largely affected by the surface and terrain characteristics. The simulated vertical profiles do not show any explicit variation at different grid resolutions in upper troposphere. Therefore a comparison for all three model domains only up to 500 hPa is shown in Figure 4.

Except for the relative humidity in d01, other meteorological parameters shown here do not reveal strong dependencies on the model resolution. The temperature ranges from 20^0C at 800 hPa to -8^0C at 500 hPa in WRF simulations as well as in the observations. Model however overestimates the relative humidity near 500hPa level in d02 and d03 on some of the days. In case of the wind speed, the model underestimates the magnitude of the wind in first few days up to 500 hPa, though qualitatively the model is able to capture the vertical profiles.

https://doi.org/10.5194/gmd-2020-12
Preprint. Discussion started: 3 March 2020

Geoscientific Model Development Discussions
Open Access

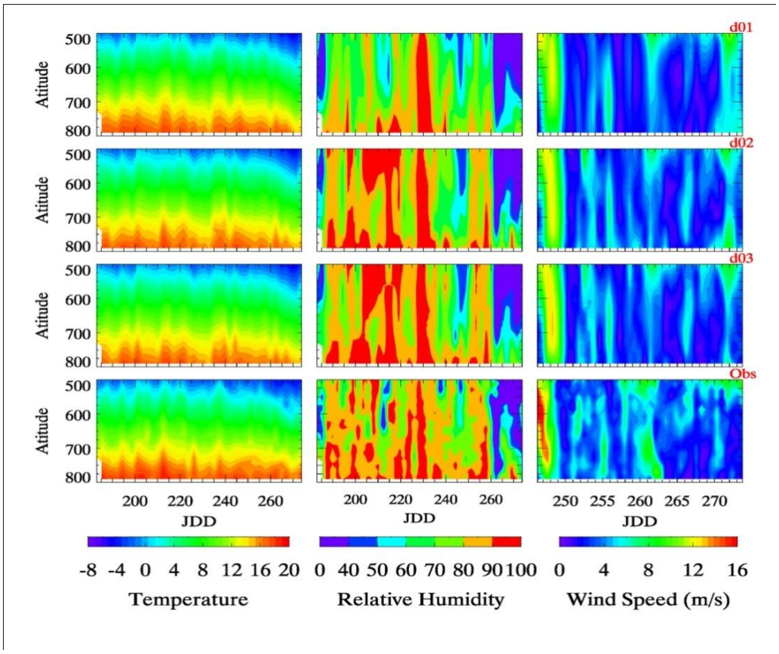

Figure 4: A comparison of temperature (first column), relative humidity (second column) and wind speed (third column) profiles for pressure range: 800 to 500 hPa for WRF simulations for all domains (d01: first row, d02: second row, d03: third row) and radiosonde observations (fourth row).

3.3. Comparison with ground-based observations

Model simulated 2m temperature, relative humidity (RH) and 10 m windspeed for the observational site, Manora Peak are compared with the ground-based measurements made during GVAX campaign in Fig.5 and summarized in Table1. The diurnal variations in 2m temperature, 2m relative humidity and 10 m wind speed simulated by the WRF model are compared with observations in Figure 5, whereas the surface pressure does not show a significant diurnal variation (not shown here). WRF model simulated 2m temperature shows warm bias in all the three domains. The simulated 2m temperature for d01 varies from 20.0 to 24.7^{0}C with the mean value of 22.3^{0}C compared to observed mean value of about 19.5±1.1^{0}C with

https://doi.org/10.5194/gmd-2020-12
Preprint. Discussion started: 3 March 2020

a correlation of r = 0.75 between d01 and observation. This warm bias is seen to decrease with increasing model resolution with bias reducing to 0.3^{0}C only for the d03 simulation.

Table1: Mean Values of the meteorological parameters during summer monsoon (JJAS)

Parameter	**Domain d01**	**Domain d02**	**Domain d03**	**Observations**
Pressure (hPa)	869.5±0.6	835.3±0.6	827.6±0.6	801.3±0.3
Temperature (^{0}C)	22.3±1.8	20.45±1.8	19.8±1.1	19.5±1.1
Relative Humidity (%)	86.8±4.9	92.7±1.3	90.8±2.0	94.5±1.5
Wind Speed (ms^{-1})	2.1±0.4	3.0±0.6	2.6±0.5	2.2±0.4

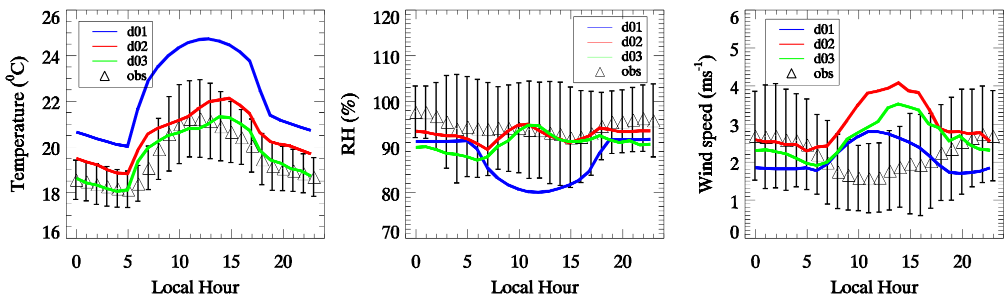

Figure 5: Mean diurnal variations in temperature, relative humidity, and wind speed from three simulations and observations.

The 10 m wind speed shows explicit trend of variation with grid resolution with finest resolution predicting nighttime wind speeds quite well. Diurnal mean wind speed is less predictable and shows an opposite trend of variation in daytime, which may be attributed to the orography induced effects. In case of the coarser resolution domain (d01), the wind speed is underestimated by 0.1 ms^{-1} while overestimated by 0.4 ms^{-1} in d03 with a poor correlation (r~0.21).

https://doi.org/10.5194/gmd-2020-12
Preprint. Discussion started: 3 March 2020

Geoscientific Model Development
Discussions

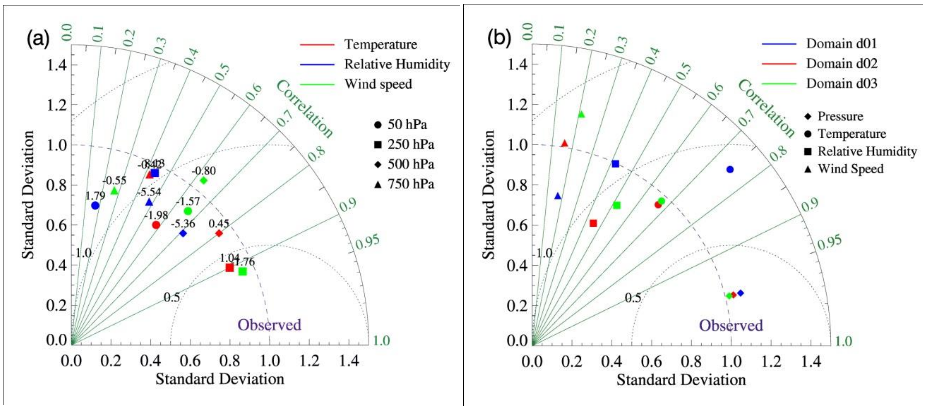

Figure 6: Taylor diagram with correlation coefficient, normalized standard deviation, and normalized root mean square difference (RMSD) error for (a) model performance at different pressure levels shown in Figure 3 and (b) the model simulated surface pressure, 2m temperature, RH and 10 m wind speed for different domains as shown in Figure 5.

The simulated relative humidity shows decreasing trend during daytime and reaches up to a minimum value of about 79.9% between 11:00 to 13:00 LST for d01. Model simulates mean relative humidity of 86.8 ± 4.9% with dry bias of 8% with moderate correlation (r = 0.42) for domain d01. The dryness in the simulated atmosphere decreases up to 3% in d03 (r = 0.52) with the increasing grid resolution. Overall, various aspects of the model performance such as normalized standard deviation, normalized root mean square difference error and the correlation with ground-based observations are summarized in form of Taylor's diagram in Figure 6b. From Table1 and Figure 6b the model simulated surface pressure shows a positive bias of 68 hPa with a good correlation of 0.97 in d01 with respect to the observed value which is about 801.3 hPa. The bias decreases up to 26 hPa in d03 i.e. the highest resolution simulation.

The normalized standard deviation of meteorological parameters as shown in Figure 6b explains that except simulated 2 m temperature in d02 and wind speed in d03, all meteorological parameters are show

https://doi.org/10.5194/gmd-2020-12
Preprint. Discussion started: 3 March 2020

lower variability. As clear from Table.1, the temperature warm biases in d02 and d03 (0.9^0C and 0.3^0C respectively) are lower as compared to the d01 (2.8^0C).

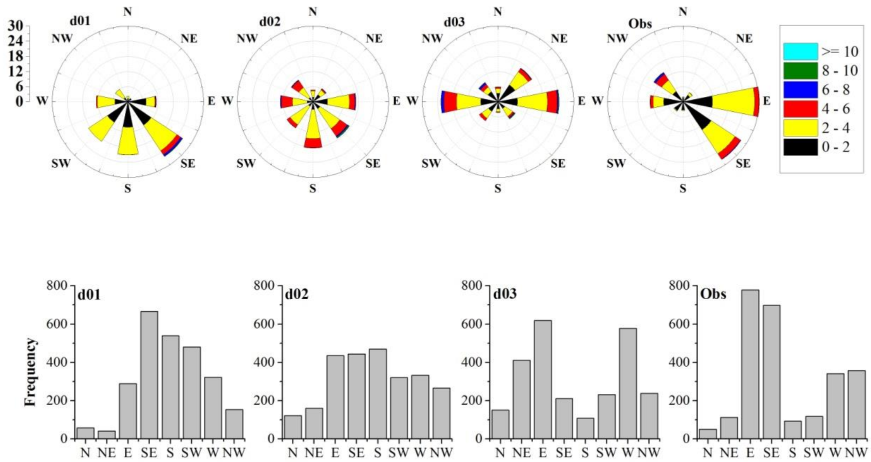

Figure 7: Comparison of the wind direction in form of (a) wind-rose diagrams and (b) frequency distribution from model simulations at three different resolution and observations

Wind directions are analysed in Figure 7 using wind-rose diagrams and frequency distribution. The winds varying between meteorological direction 337.5^0 and 22.5^0 are considered to be the Northerly and represented by N in the frequency distribution and so on for other directions taking into account the clockwise meteorological convention. Wind direction are seen to vary differently at different model resolutions. The frequency of southerly (539) and south-westerly (SW, 481) are quite higher in d01 as compared to the observations (93 and 118 respectively), which decreases up to 109 and 232 in d03. Model is able to simulate the northerly and north-easterly winds in d01 and d02, while, model simulates larger contribution of north easterly winds in d03. The dominance of the summer monsoon seasonal easterly (30%) and south-easterly (27%) winds is seen in the observation. The easterly component of the model simulated wind shows better agreement with observations on increasing the model resolution. Additionally, the model is able to simulate the westerly and north-westerly wind contribution in d02,

https://doi.org/10.5194/gmd-2020-12
Preprint. Discussion started: 3 March 2020

whereas, the westerly component is over predicted by 70% in d03. Hence, it is concluded that wind direction also shows explicit dependency on the model resolution.

3.4. Effect of feedback

In the preceding section, the results of the simulations carried out without any feedbacks (WRF-WF) from the finer resolution domain to its parent domain were presented. This WRF-WF experiment was conducted in such a way that it could explicitly account for the grid resolution effects on the model performance. The simulated meteorology with this model setup depicted different model performance in outermost coarse resolution domain d01 as compared to d02 and d03 (Fig. 2 and 5). Another model simulation is carried out in this section using the same configuration but with two-way interactive nesting and feedback (WRF-F) from daughter domain to its mother domain. The model results over CH region in the regional scale simulation (d01) shows better agreement with the observations because of the feedback from high resolution nested simulation. The comparison of the simulated meteorological parameters (2m temperature, RH, and 10 m wind speed) for outermost domain with the surface observations is presented in Figure 8 for both WRF-WF and WRF-F, and the effect of the feedback within outermost domain is given in Figure 9.

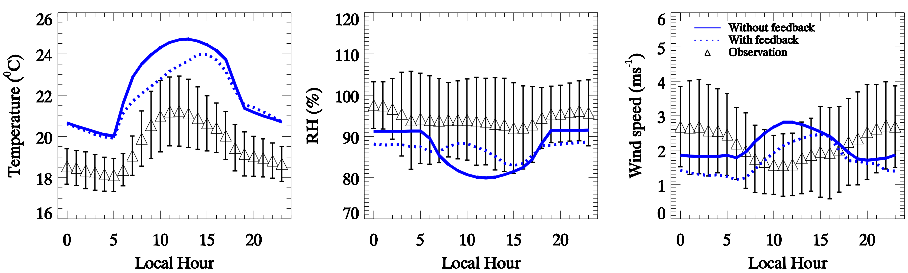

Figure 8: The diurnal variation of the 2 m temperature, relative humidity and 10 m wind speed.

https://doi.org/10.5194/gmd-2020-12
Preprint. Discussion started: 3 March 2020

Geoscientific Model Development Discussions
Open Access

The analysis of simulated meteorological parameters for observational site in WRF-WF and WRF-F experiments reveal the following:

1. The range of the diurnal variation of 2 m temperature in d01 changes from 20 – 24.7^{0}C in WRF-WF to 19.9-23.9^{0}C in WRF-F with a slight decrease in warm bias from 2.8^{0}C to 2.4^{0}C (Figure 8). This reduction in bias is the low temperature feature of the elevated terrain captured at higher resolution which is feedback to the d01.
2. For observational site, WRF-F simulated relative humidity is 86.9% which is 0.1% wetter than WRF-WF for outermost domain which is negligible. Also, WRF-F shows a different trend of variation during daytime as compared to the WRF-WF for domain d01 (Figure 8). The comparison of the WRF-WF and WRF-F simulated meteorology is compared in Table 2.
3. The effect of the feedback is more significant over the mountainous region than in the plains as evident from the Figure 9.
4. Changes akin to 2 m temperature are observed in the surface pressure in WRF-F (Table 2). The positive bias is reduced by 11 hPa. Again, the same low-pressure feature of elevated mountain peaks is identified and captured by the model through the feedback.
5. Model simulated wind speed between the two cases: WRF-WF and WRF-F shows noticeable differences, although the trend of diurnal variation remains similar. The WRF-F simulated wind speed is lower by 0.4 ms^{-1} in domain d01 as compared to WRF-WF, which is also close to the observation (2.2±0.4ms^{-1}) made during the GVAX campaign.

https://doi.org/10.5194/gmd-2020-12
Preprint. Discussion started: 3 March 2020

Geoscientific Model Development Discussions

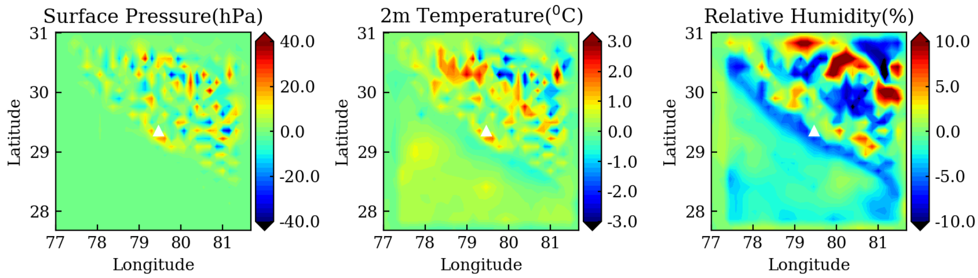

Figure 9: The effect of the two-way nesting on d01 is shown. The difference between the simulations with feedback (WRF-F) and without feedback (WRF-WF) is shown.

Table 2: Comparison of the simulated meteorology in two model simulations: WRF-WF and WRF-F at the observational site from outermost domain.

Parameters	Observed value	WRF-WF		WRF-F	
		Value	Bias	Value	Bias
Pressure (hPa)	801.3±0.3	869.5±0.6	+68.2	858.9±0.7	+57.2
Temperature (^{0}C)	19.5±1.1	22.3±1.8	+2.8	21.9±1.4	+2.4
RH (%)	94.5±1.5	86.8±4.9	-7.7	86.9±4.9	-7.6
WS (ms^{-1})	2.2±0.4	2.1±0.4	-0.1	1.7±0.4	-0.5

The feedback from the daughter domain to parent domain process mostly modifies the meteorology over the mountainous region within the domain. The effect of feedback is strikingly observed for the 2m temperature and the trend of diurnal variation of the relative humidity. Over all the model performance improved with the feedback, nevertheless further modelling studies alongside with more observations are needed to improve the model performance. Next, we implement a high resolution (3s) topographical input in the model to evaluate further fine resolution features over Himalaya.

https://doi.org/10.5194/gmd-2020-12
Preprint. Discussion started: 3 March 2020

Geoscientific Model Development
Discussions

3.5. Inclusion of high resolution (3s) SRTM topography

Simulations described in previous sections were performed using the 30s (~1km) topographic data from the GMTED2010 (Danielson and Gesch, 2011). The resolution of this (30s or ~0.95km) is comparable to the highest resolution of the WRF simulation (d03). To evaluate influences of topographical features over even finer scales on the wind flows over this highly complex terrain, topography input available at very high resolution (3s or ~90m) from the Shuttle Radar Topography Mission (SRTM3s) (Farr et al., 2007) has been implemented without altering the model configuration, except performing the simulation as d04 (~333m). Simulation with SRTM data but at 1 km resolution did not differ significantly with the similar resolution simulation using GMTED2010. For this experiment, model simulation is performed for 1 month only (September 2011). This simulation carried out without feedback and compared with the observation to check the effect of implementing high-resolution topography.

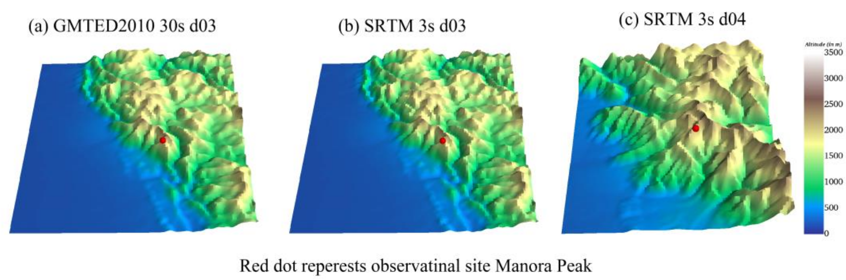

Figure 10: The topography from GMTED2010 at 30s and SRTM at 3s in domain d03 and d04.

The topography does not change much within d02 and d03 by changing input from GMTED2010 to SRTM3s (Supplementary Figure S1). The topography in the d04 get better resolved as depicted by sharp variations of mountain ridges and valleys using the SRTM3s as compared to the d03, as shown in the Figure 10, which could be smoothed out if the simulation was carried out with GMTED2010 / or at 1 km with SRTM3s. The induced effects due the more resolved topography in d04 can better simulate the local circulation of air mass. Therefore, simulated 10 m wind direction in d04 is compared with the observations

https://doi.org/10.5194/gmd-2020-12
Preprint. Discussion started: 3 March 2020

Geoscientific Model Development Discussions
Open Access

and d03 to investigate the effect of including the SRTM3s topography. Surface pressure is seen to be simulated more realistically (809 hPa) and the dry bias in 2m relative humidity is improved by ~2%.

Wind variations are shown in forms of the wind rose diagram using GMTED2010 and SRTM3s (Figure 11 and Supplementary Figure S2). The southerly wind component consistently shows an agreement with the observations with increasing model resolution. The observation shows the prevalence of north-westerly (19%), easterly (25%), westerly (18%) and south-easterly (20%) winds and these are also seen to be dominant directions in the simulation d04, while occurrence of south-easterly winds is underestimated. The least observed component is the northerly wind with (3%) while simulated by model is about 15% and 11% in d03 and d04 respectively.

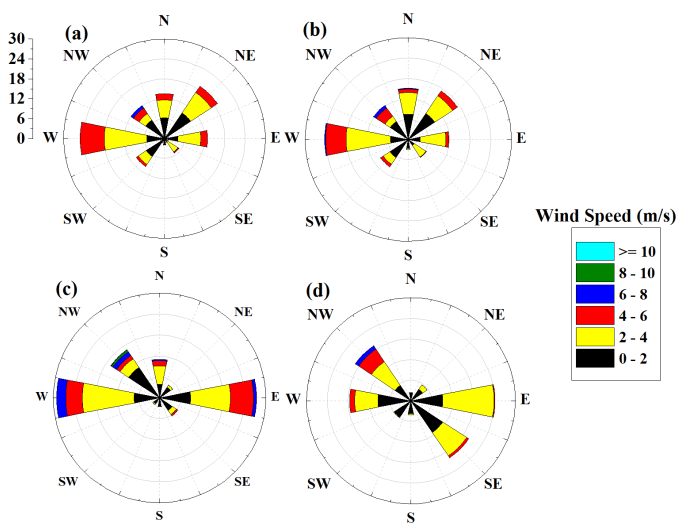

Figure 11: Wind rose diagrams for d03 using GMTED2010 (a), d03 and d04 using SRTM3s topography data in (b), (c), and observation (d).

The observed southerly wind component is 4% while simulated as (3%) in d03 and d04. Simulation of the wind directions improved from d03 to d04 by using the SRTM3s topography being relatively in better agreement with observations, except certain wind directions such as south easterly. An improvement is noticed in simulated surface pressure, 2 m relative humidity and 10 m wind speed using the SRTM3s topography over the complex CH. The effects of the SRTM3s topographic static data is studied previously over other regions of the world (e. g. Teixeira et al., 2014; De Meij and Vinuesa, 2014). The differences between model and observations of winds over the Himalayan region are suggested to be associated with still unresolved terrain features, besides the influences of input meteorological fields as well as the model physics on simulated atmospheric flows (e. g. Xue et al., 2014; Vincent et al., 2015).

4. Summary and Conclusions

In this study, the effects of spatial resolution on model simulated meteorology over the CH has been examined combining the WRF model with ground-based, balloon-borne observations during and intensive field campaign, and reanalysis datasets. Owing to the highly complex topography of the central Himalaya, model results show strong sensitivity towards the model resolution and adequate representation of terrain features. Model simulated meteorological profiles do not show much dependency on resolution except in the lower atmosphere, which is directly influenced by terrain induced effects and surface characteristics. The biases in 2 m temperature, relative humidity and pressure show a decrease on increasing the model resolution indicating a well resolved representation of topographical features. Diurnal variations in meteorological parameters also show better agreements on increasing the grid resolution. Although the surface pressure does not show a pronounced diurnal variation nevertheless the biases in simulated surface pressure reduce drastically over fine resolution simulations. Model is generally not able to reproduce the wind directions well, except some of the major components in all the simulations with varying resolutions. A sensitivity experiment with domain feedback turned ON shows that the feedback process can improve the representation of the CH in the simulation covering larger region of the northern Indian subcontinent. It is suggested that further improvements in the model performance are limited due to the lack of high-resolution topographical inputs, biases through input meteorological fields, and model physics.

https://doi.org/10.5194/gmd-2020-12
Preprint. Discussion started: 3 March 2020

Geoscientific Model Development Discussions
Open Access

Nevertheless, an implementation of a very high resolution (3s) topographical input using the SRTM data shows potential to reduce the biases related to topographical features to some extent.

Code and data availability

WRF is an open-source and publicly available model, which can be downloaded at http://www2.mmm.ucar.edu/wrf/users/download/get_source.html. Observations from the GVAX field campaign are also available freely (https://adc.arm.gov/discovery/#v/results/s/fsite::pgh.M).

Author contributions

NS and AP designed and supervised the study. JS performed the simulations, assisted by NO and AS. JS, NO, AS analysed the model results and NVPKK, KR, SSG contributed to the interpretations. VRK contributed significantly in conceiving and realizing the GVAX campaign. JS and NS wrote the first draft, and all the authors contributed to the manuscript.

Acknowledgement

This study has been supported by ABLN& C: NOBLE project under ISRO-GBP. We are thankful to Director ARIES, Nainital. We acknowledge NCAR for the WRF-ARW model, ECMWF for the ERA-Interim reanalysis data sets, ARM Climate Research Facility of U.S. Department of Energy (DOE) for availing the observations made during GVAX campaign. Computing resources from the Max Planck Computing and Data Facility (MPCDF) are acknowledged. N. Ojha acknowledges the computing resources - Vikram-100 HPC at Physical Research Laboratory (PRL), and valuable support from Duggirala Pallamraju and Anil Bhardwaj.

https://doi.org/10.5194/gmd-2020-12
Preprint. Discussion started: 3 March 2020

References

Bhutiyani, M.R., Kale, V.S. and Pawar, N.J.: Long-term trends in maximum, minimum and mean annual air temperatures across the Northwestern Himalaya during the twentieth century. Climatic Change, *85*, 59-177,https://doi.org/10.1007/s10584-006-9196-1.,2007.

Bonasoni, P., Cristofanelli, P., Marinoni, A., Vuillermoz, E. and Adhikary, B.: Atmospheric pollution in the Hindu Kush–Himalaya region: Evidence and implications for the regional climate. Mountain research and development, 32, 468-479, 2012.

Boyle, J. and Klein, S.A.: Impact of horizontal resolution on climate model forecasts of tropical precipitation and diabatic heating for the TWP-ICE period. Journal of Geophysical Research: Atmospheres, 115, https://doi.org/10.1029/2010JD014262, 2010.

Caya, D. and Laprise, R.: A semi-implicit semi-Lagrangian regional climate model: The Canadian RCM. Monthly Weather Review, 127, 341-362, https://doi.org/10.1175/1520-0493(1999)127<0341:ASISLR>2.0.CO;2, 1999.

Chen, F. and Dudhia, J.: Coupling an advanced land surface–hydrology model with the Penn State–NCAR MM5 modeling system. Part I: Model implementation and sensitivity. Monthly Weather Review, 129, 569-585,https://doi.org/10.1175/1520-0493(2001)129<0569:CAALSH>2.0.CO;22001.

Chen, F., Kusaka, H., Bornstein, R., Ching, J., Grimmond, C.S.B., Grossman-Clarke, S., Loridan, T., Manning, K.W., Martilli, A., Miao, S. and Sailor, D.: The integrated WRF/urban modelling system: development, evaluation, and applications to urban environmental problems, International Journal of Climatology, 31, 273-288, https://doi.org/10.1002/joc.2158, 2011.

Chou, M.D. and Suarez, M.J.: An efficient thermal infrared radiation parameterization for use in general circulation models, NASA Technical Memorandum No. 104606, Vol. 3, pp.85,1994.

https://doi.org/10.5194/gmd-2020-12
Preprint. Discussion started: 3 March 2020

Geoscientific Model Development Discussions
Open Access

Christensen, J.H., Christensen, O.B., Lopez, P., van Meijgaard, E. and Botzet, M.: The HIRHAM4 regional atmospheric climate model.DMI Scientific report, 4, p.51, 1996.

Danielson, J.J. and Gesch, D.B.: Global multi-resolution terrain elevation data 2010 (GMTED2010) (No. 2011-1073), US Geological Survey, 2011.

De Meij, A. and Vinuesa, J. F.: Impact of SRTM and Corine Land Cover data on meteorological parameters using WRF, Atmos. Res., 143, 351–370, doi:10.1016/j.atmosres.2014.03.004, 2014.

Dee, D.P., Uppala, S.M., Simmons, A.J., Berrisford, P., Poli, P., Kobayashi, S., Andrae, U., Balmaseda, M.A., Balsamo, G., Bauer, D.P. and Bechtold, P.: The ERA-Interim reanalysis: Configuration and performance of the data assimilation system. Quarterly Journal of the royal meteorological society, 137, pp.553-597, https://doi.org/10.1002/qj.828, 2011.

Deep, A., Pandey, C.P., Nandan, H. et al. Evaluation of ambient air quality in Dehradun city during 2011–2014. J Earth Syst Sci 128, 96 (2019) doi:10.1007/s12040-019-1092-y

Dimri, A.P., Chevuturi, A., Niyogi, D., Thayyen, R.J., Ray, K., Tripathi, S.N., Pandey, A.K. and Mohanty, U.C.: Cloudbursts in Indian Himalayas: a review. Earth-science reviews, 168, pp.1-23, https://doi.org/10.1016/j.earscirev.2017.03.006, 2017.

Ek, M.B., Mitchell, K.E., Lin, Y., Rogers, E., Grunmann, P., Koren, V., Gayno, G. and Tarpley, J.D.: Implementation of Noah land surface model advances in the National Centers for Environmental Prediction operational mesoscale Eta model. Journal of Geophysical Research: Atmospheres, https://doi.org/10.1029/2002JD003296, 2003.

Farr, T.G., Rosen, P.A., Caro, E., Crippen, R., Duren, R., Hensley, S., Kobrick, M., Paller, M., Rodriguez, E., Roth, L. and Seal, D.: The shuttle radar topography mission, Reviews of geophysics, 45(2). doi:10.1029/2005RG000183, 2007.

https://doi.org/10.5194/gmd-2020-12
Preprint. Discussion started: 3 March 2020

Geoscientific Model Development Discussions
Open Access

Foley, A.M.: Uncertainty in regional climate modelling: A review. Progress in Physical Geography, 34, pp.647-670.https://doi.org/10.1177/0309133310375654, 2010.

Hong, S.Y., Noh, Y. and Dudhia, J.: A new vertical diffusion package with an explicit treatment of entrainment processes. Monthly weather review, 134, pp.2318-2341, https://doi.org/10.1175/MWR3199.1, 2006.

Jiménez, P.A., Dudhia, J., González-Rouco, J.F., Navarro, J., Montávez, J.P. and García-Bustamante, E.: A revised scheme for the WRF surface layer formulation. Monthly Weather Review, 140, pp.898-918.https://doi.org/10.1175/MWR-D-11-00056.1, 2012.

Kain, J.S.: The Kain–Fritsch convective parameterization: an update. Journal of applied meteorology, 43, pp.170-181, https://doi.org/10.1175/1520-0450(2004)043<0170:TKCPAU>2.0.CO;2 ,2004.

Kotamarthi, V.R.: Ganges Valley Aerosol Experiment (GVAX) Final Campaign Report. DOE/SC-ARM-14-011, available at: https://www. arm. gov/publications/programdocs/doe-sc-arm-14-011. Pdf, 2013.

Kumar, R., Naja, M., Pfister, G.G., Barth, M.C. and Brasseur, G.P.: Simulations over South Asia using the Weather Research and Forecasting model with Chemistry (WRF-Chem): set-up and meteorological evaluation. Geoscientific Model Development, 5, p.321, https://doi.org/10.5194/gmd-5-321-2012, 2012

Laprise, R. Regional climate modelling. Journal of Computational Physics, 227, pp.3641-3666., https://doi.org/10.1016/j.jcp.2006.10.024, 2008.

Lawrence, M.G. and Lelieveld, J.: Atmospheric pollutant outflow from southern Asia: a review. Atmospheric Chemistry and Physics, 10, p.11017, https://doi.org/10.5194/acp-10-11017-2010, 2010.

Lelieveld, J., Bourtsoukidis, E., Brühl, C., Fischer, H., Fuchs, H., Harder, H., Hofzumahaus, A., Holland, F., Marno, D., Neumaier, M. and Pozzer, A.: The South Asian monsoon—pollution pump and purifier. Science, 361, pp.270-273, DOI:10.1126/science.aar2501, 2018.

Meher, J.K., Das, L., Akhter, J., Benestad, R.E. and Mezghani, A.: 2017. Performance of CMIP3 and CMIP5 GCMs to simulate observed rainfall characteristics over the Western Himalayan region.Journal of Climate, 30, pp.7777-7799,*https://doi.org/10.1175/JCLI-D-16-0774.1*, 2017.

Mlawer, E.J., Taubman, S.J., Brown, P.D., Iacono, M.J. and Clough, S.A.: Radiative transfer for inhomogeneous atmospheres: RRTM, a validated correlated-k model for the longwave. Journal of Geophysical Research: Atmospheres, 102, pp.16663-16682. https://doi.org/10.1029/97JD00237, 1997.

Mues, A., Lauer, A., Lupascu, A., Rupakheti, M., Kuik, F. and Lawrence, M.G.: WRF and WRF-Chem v3. 5.1 simulations of meteorology and black carbon concentrations in the Kathmandu Valley. Geoscientific Model Development, 11, p.2067. https://doi.org/10.5194/gmd-11-2067-2018, 2018.

Naja, M., Bhardwaj, P., Singh, N., Kumar, P., Kumar, R., Ojha, N., Sagar, R., Satheesh, S. K., Krishna Moorthy, K., Kotamarthi, V. R., High-frequency vertical profiling of meteorological parameters using AMF1 facility during RAWEX–GVAX at ARIES, Nainital, Current Science, Vol. 111, No. 1, 132–140, 2016.

Nandargi, S. and Dhar, O.N.: Extreme rainstorm events over the northwest Himalayas during 1875–2010. Journal of Hydrometeorology, https://doi.org/10.1175/JHM-D-12-08.1 ,2012.

Ojha, N., Naja, M., Singh, K.P., Sarangi, T., Kumar, R., Lal, S., Lawrence, M.G., Butler, T.M. and Chandola, H.C.: Variabilities in ozone at a semi-urban site in the Indo-Gangetic Plain region: Association with the meteorology and regional processes. Journal of Geophysical Research: Atmospheres, https://doi.org/10.1029/2012JD017716, 2012.

Ojha, N., Pozzer, A., Rauthe-Schöch, A., Baker, A.K., Yoon, J., Brenninkmeijer, C.A. and Lelieveld, J.: Ozone and carbon monoxide over India during the summer monsoon: regional emissions and transport. Atmos. Chem. Phys, https://doi.org/10.5194/acp-16-3013-2016, 2016.

https://doi.org/10.5194/gmd-2020-12
Preprint. Discussion started: 3 March 2020

Ojha, N., Girach, I., Sharma, K., Nair, P., Singh, J., Sharma, N., Singh, N., Flemming, J., Inness, A. and Subrahmanyam, K.V.: Surface ozone in the Doon Valley of the Himalayan foothills during spring. Environ. Sci. Poll. Res., doi:10.1007/s11356-019-05085-2, 2019

Pal, J.S., Giorgi, F., Bi, X., Elguindi, N., Solmon, F., Gao, X., Rauscher, S.A., Francisco, R., Zakey, A., Winter, J. and Ashfaq, M.: Regional climate modeling for the developing world: the ICTP RegCM3 and RegCNET. Bulletin of the American Meteorological Society, https://doi.org/10.1175/BAMS-88-9-1395, 2007.

Palazzi, E., von Hardenberg, J., Terzago, S. and Provenzale, A.: Precipitation in the Karakoram-Himalaya: a CMIP5 view. Climate Dynamics, 45, pp.21-45, https://doi.org/10.1007/s00382-014-2341-z, 2015.

Pant, G.B., Pradeep Kumar, P., V. Revadekar, Jayashree, Singh, Narendra.: The Himalaya. https://doi.org/10.1007/978-3-319-61654-4, 2018.

Pant, P., Hegde, P., Dumka, U.C., Sagar, R., Satheesh, S.K., Moorthy, K.K., Saha, A. and Srivastava, M.K.: Aerosol characteristics at a high-altitude location in central Himalayas: Optical properties and radiative forcing. Journal of Geophysical Research: Atmospheres. https://doi.org/10.1029/2005JD006768, 2006.

Pervez, M.S. and Henebry, G.M.: Projections of the Ganges–Brahmaputra precipitation—Downscaled from GCM predictors. Journal of Hydrology, 517, pp.120-134.https://doi.org/10.1016/j.jhydrol.2014.05.016, 2014

Rupakheti, D., Adhikary, B., Praveen, P.S., Rupakheti, M., Kang, S., Mahata, K.S., Naja, M., Zhang, Q., Panday, A.K. and Lawrence, M.G., 2017.: Pre-monsoon air quality over Lumbini, a world heritage site along the Himalayan foothills. Atmos. Chem. Phys., 17, 11041-11063, https://doi.org/10.5194/acp-17-11041-2017, 2017.

Sarangi, T., Naja, M., Ojha, N., Kumar, R., Lal, S., Venkataramani, S., Kumar, A., Sagar, R. and Chandola, H.C.: First simultaneous measurements of ozone, CO, and NOy at a high-altitude regional representative site in the central Himalayas. Journal of Geophysical Research: Atmospheres, 119, pp.1592-1611. https://doi.org/10.1002/2013JD020631, 2014.

Sharma, S.S. and Ganju, A.: Complexities of avalanche forecasting in Western Himalaya—an overview. *Cold Regions Science and Technology*, *31*, pp.95-102.https://doi.org/10.1016/S0165-232X(99)00034-8, 2000.

Sharma, A., Ojha, N., Pozzer, A., Mar, K. A., Beig, G., Lelieveld, J., and Gunthe, S. S.: WRF-Chem simulated surface ozone over south Asia during the pre-monsoon: effects of emission inventories and chemical mechanisms, Atmos. Chem. Phys., 17, 14393–14413, https://doi.org/10.5194/acp-17-14393-2017, 2017.

Singh, N., Solanki, R., Ojha, N., Janssen, R.H., Pozzer, A. and Dhaka, S.K.: Boundary layer evolution over the central Himalayas from radio wind profiler and model simulations. Atmospheric Chemistry & Physics, https://doi.org/10.5194/acp-16-10559-2016, 2016.

Singh, N., Solanki, R., Ojha, N., Naja, M., Dumka, U. C., Phanikumar, D. V., Sagar, R., Satheesh, S. K., Krishna Moorthy, K., Kotamarthi, V. R., Dhaka, S. K.: Variations in the cloud-base height over the central Himalayas during GVAX: association with the monsoon rainfall, Current Science, volume 111, pp. 109-116, 2016.

Skamarock, W. C.,Klemp, J.B., Dudhia, J., Gill, D.O., Barker, D.M., Wang, W. and Powers, J.G.: A Description of the Advanced Research WRF Version 3. NCAR Technical Note NCAR/TN-475+STR, http://dx.doi.org/10.5065/D68S4MVH,, 2008.

Solanki, R., Singh, N., Kumar, N.K., Rajeev, K. and Dhaka, S.K.: Time variability of surface-layer characteristics over a mountain ridge in the central Himalayas during the spring season. Boundary-layer meteorology, 158, pp.453-471, https://doi.org/10.1007/s10546-015-0098-5, 2016.

https://doi.org/10.5194/gmd-2020-12
Preprint. Discussion started: 3 March 2020

Geoscientific Model Development Discussions

Srivastava, A.K., Ram, K., Pant, P., Hegde, P. and Joshi, H.: Black carbon aerosols over Manora Peak in the Indian Himalayan foothills: implications for climate forcing. Environmental Research Letters, 7, p.014002, 2012.

Sun, X.B., Ren, G.Y., Shrestha, A.B., Ren, Y.Y., You, Q.L., Zhan, Y.J., Xu, Y. and Rajbhandari, R.: Changes in extreme temperature events over the Hindu Kush Himalaya during 1961–2015. Advances in Climate Change Research, https://doi.org/10.1016/j.accre.2017.07.001, 2017.

Taylor, K.E.: Summarizing multiple aspects of model performance in a single diagram. Journal of Geophysical Research: Atmospheres, 106, pp.7183-7192, https://doi.org/10.1029/2000JD900719, 2001.

Teixeira, J. C., Carvalho, A. C., Carvalho, M. J., Luna, T. and Rocha, A.: Sensitivity of the WRF model to the lower boundary in an extreme precipitation event-Madeira island case study, Nat. Hazards Earth Syst. Sci., 14(8), 2009–2025, doi:10.5194/nhess-14-2009-2014, 2014.

Tewari, M., Chen, F., Wang, W., Dudhia, J., LeMone, M.A., Mitchell, K., Ek, M., Gayno, G., Wegiel, J. and Cuenca, R.H.: Implementation and verification of the unified NOAH land surface model in the WRF model. In 20th conference on weather analysis and forecasting/16th conference on numerical weather prediction (Vol. 1115) , 2004,

Thompson, G., Rasmussen, R.M. and Manning, K.: Explicit forecasts of winter precipitation using an improved bulk microphysics scheme. Part I: Description and sensitivity analysis. Monthly Weather Review, 132(2), pp.519-542,https://doi.org/10.1175/1520-0493(2004)132<0519:EFOWPU>2.0.CO;2, 2004.

Tiwari, P.R., Kar, S.C., Mohanty, U.C., Dey, S., Sinha, P. and Shekhar, M.S.: Sensitivity of the Himalayan orography representation in simulation of winter precipitation using Regional Climate Model (RegCM) nested in a GCM. Climate Dynamics, 49(11-12), pp.4157-4170, https://doi.org/10.1007/s00382-017-3567-3, 2017.

https://doi.org/10.5194/gmd-2020-12
Preprint. Discussion started: 3 March 2020

Geoscientific Model Development Discussions
Open Access

Tselioudis, G., Douvis, C. and Zerefos, C.: Does dynamical downscaling introduce novel information in climate model simulations of precipitation change over a complex topography region? International Journal of Climatology, 32, pp.1572-1578,https://doi.org/10.1002/joc.2360, 2012.

Vincent, C. L. and Hahmann, A. N.: The impact of grid and spectral nudging on the variance of the near-surface wind speed, J. Appl. Meteorol. Climatol., 54(5), 1021–1038, doi:10.1175/JAMC-D-14-0047.1, 2015.

Wang, Y., Leung, L.R., McGREGOR, J.L., Lee, D.K., Wang, W.C., Ding, Y. and Kimura, F.: Regional climate modeling: progress, challenges, and prospects. Journal of the Meteorological Society of Japan. Ser. II, 82, pp.1599-1628,https://doi.org/10.2151/jmsj.82.1599, 2004.

Weisman, M.L., Skamarock, W.C. and Klemp, J.B.: The resolution dependence of explicitly modeled convective systems. Monthly Weather Review, 125, pp.527-548, https://doi.org/10.1175/1520-0493(1997)125<0527:TRDOEM>2.0.CO;2, 1997.

Wilby, R.L., Hay, L.E. and Leavesley, G.H.: A comparison of downscaled and raw GCM output: implications for climate change scenarios in the San Juan River basin, Colorado. Journal of Hydrology, 225, pp.67-91, https://doi.org/10.1016/S0022-1694(99)00136-5, 1999.

Xue, Y., Janjic, Z., Dudhia, J., Vasic, R. and De Sales, F.: A review on regional dynamical downscaling in intraseasonal to seasonal simulation/prediction and major factors that affect downscaling ability, Atmos. Res., 147–148, 68–85, doi:10.1016/j.atmosres.2014.05.001, 2014.

Zadra, A., Caya, D., Côté, J.E.A.N., Dugas, B., Jones, C., Laprise, R., Winger, K. and Caron, L.P.: The next Canadian regional climate model. PhysCan, 64, pp.75-83, 2008.